Slov Vet Res 2021; 58 (Suppl 24): 177–86
DOI 10.26873/SVR-1438-2021

Original Research Article

ISOLATION AND CHARACTERIZATION OF FETAL AND NEONATAL LIVER-DERIVED MESENCHYMAL STEM CELLS FROM RABBITS

Esraa M. M. Elsheikh[1]*, Enas EL-Hady[1], Somia H. Abdallah[2], Atef A. A. E. Selem[1], Mervat M. H. Konsowa[1]*

[1]Anatomy and Embryology Department, Faculty of Veterinary Medicine, [2]Biochemistry and Molecular Biology Department, Faculty of Medicine, Zagazig University, Egypt

*Corresponding Authors, E-mail: eelsheikh41@gmail.com, mmkonsoa@vet.zu.edu.eg

Abstract: Mesenchymal stem cells (MSCs) became in recent years a promising implement for cell therapies. Our study described the isolation and characterization of liver mesenchymal stem cells (LMSCs). We isolated LMSCs from the rabbit liver tissue from two groups: 20th day's old fetuses and 4 days-old kittens. LMSCs were characterized by flow cytometry, immunohistochemistry (IHC), and quantitative real-time-polymerase chain reaction (qRT-PCR). Flow cytometry of the isolated LMSCs showed variable expression of the cluster of differentiation markers (CD) including, CD105, CD106, CD11b, CD38, CD63, CD9, and CD14. Fetal liver isolated LMSCs showed expression of CD105, CD106, CD9, and CD63 but no expression of CD14, CD11b, and CD38 was observed. Absolute expression of LMSCs was performed by qRT-PCR analysis to detect cytoskeleton genes including, vimentin, nestin, and desmin in the experimental groups. In vivo localization of stem cell markers such as CD105 (Endoglin), vimentin, and desmin was also distinguished in fetal and neonatal liver tissues using IHC.

Key words: liver; mesenchymal stem cells; immunohistochemistry; flow cytometry; rabbit

Introduction

Stem cells were specialized cells that had the capability of self-renewal. They produced daughter cells that reserved the same characteristics as their progenitor cells (1). MSCs became a common source for organ transplantation because they had the probability to differentiate along many lineages, their lower immunogenicity, and possess a low oncogenic potential (2). When comparing MSCs isolated from adult rabbit bone marrow and fetal LMSCs, the latter had a superior growth rate, clonogenic competency, and plastic adherence. Recent studies showed that using fetal liver cells in liver therapies and transplantation with a higher proliferation capacity than adult tissue cells (3).

MSCs/stromal stem cells were first isolated from the bone marrow (4). Although the bone marrow was considered the common source for MSCs, they could be isolated from other sources, taking into consideration the differences in surface markers, proliferation rates, and differentiation ability. Many types of research were directed to isolate and characterize LMSCs to draw attention to the liver as an alternative source for MSCs, particularly due to increase demand for liver therapies and transplantation (4). LMSCs exhibited a distinct morphology and expressed specific sets of CD molecules. Flow cytometry and single cell-based assays were reliable to characterize these cells. The phenotypic pattern to identify the MSCs cells required expression of CD73, CD90, and CD105 and lack of CD14, CD34, CD45 (5), (6), (7) besides CD29, CD44, CD146, and CD140 (8). Immunofluorescence or immunohistochemistry was applied to determine the immune-phenotype of liver hepatic stem cells, with confirmation by either RT-PCR or immune-blotting (9).

This work showed the isolation of LMSCs from rabbits to highlight the importance of the liver as an alternative source of MSCs for liver therapies and transplantation. In vivo localization of LMSCs by IHC gave an indication for importance of these cells in liver development.

Received: 22 September 2021
Accepted for publication: October 2021

Material and methods

The research protocol was reviewed by the Institutional Animal Care and Use Committee, Zagazig University (No, ZU-IACUC/2/F/13/2021). All surgical approaches were performed under general anesthesia, and all efforts were made to minimize animal pain.

Collection of liver samples

20th day's old fetuses were harvested from 8 white New-Zealand pregnant does (weight, 2-4.5 kg, and age, 1.5-3 years) and collected from the Faculty of Veterinary Medicine and Faculty of Agriculture, Zagazig University farms. The pregnant does were anesthetized with an intramuscular injection of 35 mg/kg ketamine Hcl (KETALAR, 100mg/ml, Pfizer, NY) and 5 mg/kg xylazine (Xylaject, 20mg/ml, ADWIA, Egypt). After laparotomy, the intact fetal sacs were collected in normal isotonic saline containers and transported to the laboratory within 4–8 hours in the icebox. Under the laminar flow cabinet, the extracted fetal livers were washed with phosphate-buffered saline (PBS) (Biowest, USA) containing penicillin-streptomycin sterile-filtered solution 100ml (Biowest, USA). The same previous procedures were performed on 8 neonatal 4 day's old kittens.

Isolation and culture of rabbit LMSCs

The liver samples were the moved into 100mm culture dishes, and the enzyme reaction was dismissed by pooling the liver into 10 mL of high glucose Dulbecco's modified Eagle medium (DMEM) (Cegrogen-biotech, Germany). After mechanical disintegration of the liver tissues, the liver homogenate was digested with 16 ml trypsin 0.25% and collagenase type IV 0.1% (Sigma, USA) for about 15 min at 37°. The reaction was ended by adding an equal volume of complete DMEM. The cellular suspension was filtered through a 200µm pore size nylon mesh filter to remove cellular undigested tissues and then centrifuged at 5000 rpm/3 min and the cell pellet was washed with 20 mL of PBS. Finally, the cells were re-suspended in a complete expansion medium of DMEM containing 20% fetal bovine serum (FBS) (Biowest, South America), 1% penicillin/streptomycin, 1% L-glutamine, and 2.5 µg/mL amphotericin. The cells were then seeded overnight in 75cm² plastic screw-capped-culture flasks at 37°C in a humid 5% CO_2 incubator. LMSCs were propagated in culture for 5-7 days, replacing the culture medium every 2 days, until 90% confluent. The culture flasks were examined with an inverted microscope (LEICA DMi 1, 20 and 40xs, Germany). At confluence, cells were washed by PBS and detached with 0.25% trypsin-EDTA (Cegrogen-biotech, Germany). The viability of cell suspensions was determined by mixing 100 µl cell suspensions with 100 µl of 0.4% trypan blue solution (Lonza, USA). The previous steps were performed according to (10) and (11) methods.

qRT-PCR

Total RNA was extracted for gene expression of LMSCs from the cultured cells according to the user′s manual of the easy-RED Total RNA Extraction Kit for Liquid Samples (iNtRON Biotechnology, South Korea). After extraction, RNA was quantified using a NanoDrop (Thermo Scientific, USA). First-strand cDNA was synthesized using iScript™ cDNA Synthesis Kit-Bio-Rad according to the manufacturer's instructions and subsequently diluted with nuclease-free water to 10 ng/mL cDNA. Firstly we made Pooling of cdna of different samples for the same gene. Then we prepared serial dilution of the pooled cdna as 1/10, 1/100, 1/1000, 1/10000, and 1/100000. After that, standard curve was plotted and Y axis represented the dilution rate and X for ct value. We calculated the number of copies of the unknown samples form the standard curve with a regression model. qRT-PCR amplification mixtures (25 μL) containing 25 ng template cDNA, master mix buffer (12.5 μL); (TOPreal™ qPCR 2X PreMIX, SYBR Green with low ROX); (Enzynomics, Korea), and 300 nM forward and reverse primers were run in duplicate and performed on a QIAGEN RT-PCR (Rotor-Gene Q, QIAGEN, USA) by using Rotor-Gene Q Series software. The sequence of primers and the size of fragments in the gene bank are listed in table (1).

Flow Cytometry

A single-cell suspension with cell aliquots (5×10^4 cells in 500 µl of FACS buffer) stained with conjugated specific antibodies was incubated for 20 min at 4°C in micro-titer plates. The staining method was done under the instruction leaflet that accompanied the antibody. Cells were

washed twice with the washing buffer and analyzed by a FACScan flow cytometer (FACSort, Becton Dickinson, Germany) for one-color analysis. Data were analyzed using Cell Quest Pro software. As anti-rabbit-specific antibodies were commercially unavailable, anti-human or anti-mouse antibodies were purchased and tested for immune reactivity in rabbit cells. LMSc were directly stained with Anti-hCD9M PE-conjugated, Anti-mCD105 FITC-conjugated, Anti-hCD63 PE-conjugated, Anti-VCAM-1/CD106 FITC-conjugated, Anti-CD11b/Integrin alpha M PE-conjugated, Anti-CD14 PE-conjugated, and Anti-CD38 PE-conjugated (all from R&D systems, Minneapolis, United States). Goat anti-rabbit polyclonal IgG antibody (10 µL/10^6 cells) was used to block nonspecific antibody binding.

Immunohistochemistry

Eight liver specimens fixed in formalin or Bouin's solution were used in this study. Sliced 5-7µm paraffin wax-embedded liver sections were mounted on glass slides, then de-paraffinized and re-hydrated by graded alcohol, as previously described by (12). To retrieve the antigen, the liver sections were kept in citrate buffer (PH 6.0) microwave digestion. Endogenous peroxidase was blocked with 0.05% hydrogen peroxide-methanol solution for 30 min. To block the non-specific staining, sections were incubated in 5% normal goat serum (diluted by 1:20 PBS) for 1 hour. The slides were incubated overnight at 4 ℃ with anti-CD105 unconjugated Polyclonal, anti-Vimentin (V9) unconjugated monoclonal, and anti-Desmin unconjugated monoclonal antibodies (all from Invitrogen, Thermo Fisher Scientific). Diamino-benzidine (DAB) was used as a chromogenic substance (brown in color). All sections were counter-stained with hematoxylin. Image Analysis Slides were digitalized using Olympus digital camera (Olympus LC20- Japan) installed on Olympus microscope (Olympus BX-50, Tokyo, Japan) with 1/2X photo adaptor, using 20x and 40x objectives. The result images were analyzed on Intel® Core I3® based computer using Video Test Morphology 5.2 software (Russia) with a specific built-in routine for IHC analysis and stain quantification. Images from five slices per tissue were taken 200 µm apart. Five visions per slice were randomly chosen for assessment of positive cells using image analysis software (JID801D).

Statistical analysis

Data were expressed as mean values ± standard deviation (SD). The unpaired Student's t-test was employed to assess statistically significant differences among the samples in the qRT-PCR in fetal and neonatal groups, with a significance level set at $P \leq 0.01$.

Results and discussion

Isolation and culture of fetal and neonatal LMSCs

LMSCs were maintained in DMEM supplemented with 20% FBS. Within 24 h after seeding, the LMSCs attached to the culture flasks and started spreading. In the first days of culture, the LMSCs grew as small spherical shaped-colonies before reaching the confluence (Fig.1).

After successive culture and enrichment by complete media in culture flasks, plastic adherent cells with fibroblastic (spindle) shape proliferated on the third day of culture. Upon reaching the fifth day of culture, we found the culture flasks containing a high number of elongated fibroblastic (spindle-shaped) cells and a low count of rounded cells (Fig.1).

The previous observation showed high proliferation and growth of LMSCs in the medium, especially cells of the fetal liver source. From the foregoing findings, we noticed the classification of the LMSCs into three patterns in cell culture; small spherical shaped cells, colony-like aggregations, and a spindle-shaped or fibroblast-like morphology. These findings were like the previously reported findings in rabbits (3), (12), and (13) and (11) in humans.

When applying the viability test of rabbit LMSCs, we found that they were negatively stained for trypan blue dye, so they appeared as white shining cells. Living cells could pump out this dye and be thus negatively stained (Fig.1). We performed this test once cells were harvested, after 5 days of culture and showed the confluence of living cells (over 90%). The rapid proliferation rate of these cells indicated their importance in liver transplantation. In humans, (11) confirmed our result but, they said that the confluence of the cells was got after 7–10 days of culture.

Table 1: The primer sequences used for qRT-PCR analysis

Gene	Size (base pairs)	primers sequences [forward (F) and reverse (R)]
Vimentin	136 bp	F:5′- TGGACATTGAGATCGCCACC-3′ R:5′-GAGTGGGTGTCAACCAGAGG-3′
Desmin	186 bp	F:5′- TTTGGCACCAAGGGCTCC-3′ R:5′-CAGGAACTCCTGGTTCACGG-3′
Nestin	173 bp	F:5′-TTCCGGCTCAGAGGAAGAGT-3′ R:5′-CACCCCCATTCACATGCTCT-3′

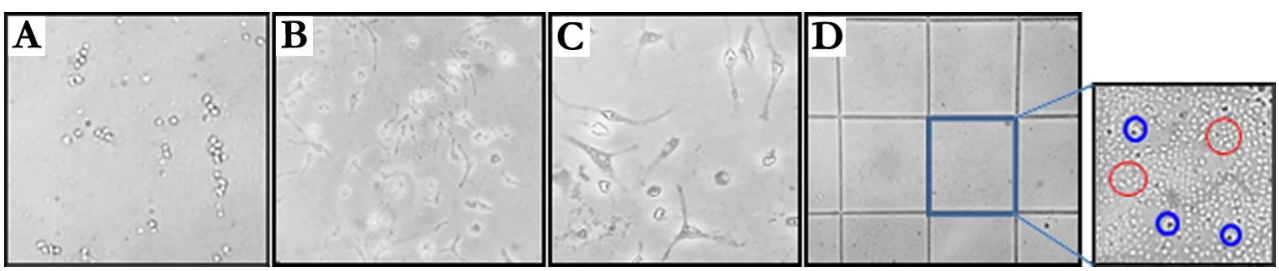

Figure 1: (A) Showing 2nd day of culture inverted microscopy of LMSCs isolated from fetal liver. (B), (C) Showing 5th day of culture inverted microscopy of fetal LMSCs (C) was the magnification power of (B). (D) Showing viability of LMSCs. Blue circle: dead cells. Red circle: live cells. The magnification power of (A) was L20× and (B), (C), and (D) was L40×

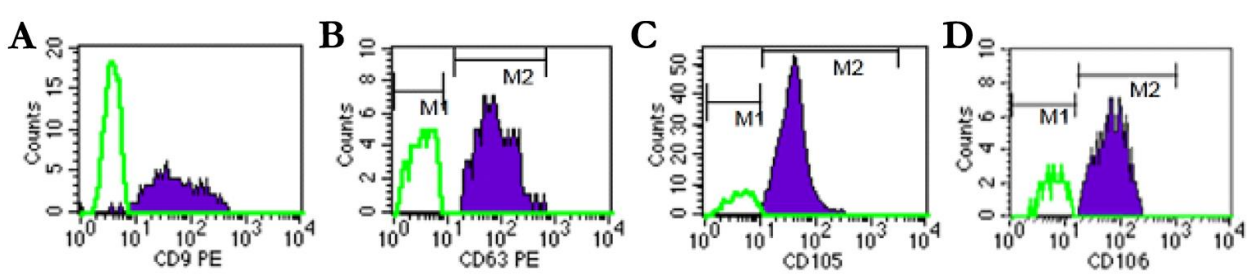

Figure 2: Representative histograms of flow cytometric analysis of fetal LMSCs. Violet filled curve represented positive cells for specific staining and non-filled line represented the negative control group. M1 referred to population 1 and M2 was population 2. (A) Cells were immunostained with CD9-PE (positive) and CD11b-PE (negative). (B) Cells were immunostained with CD63-PE (positive) and CD14-PE (negative). (C) Cells were immunostained with CD105-FITC (positive) and CD38-PE (negative). (D) Cells were immunostained with CD106-FITC (positive) and CD11b-PE (negative)

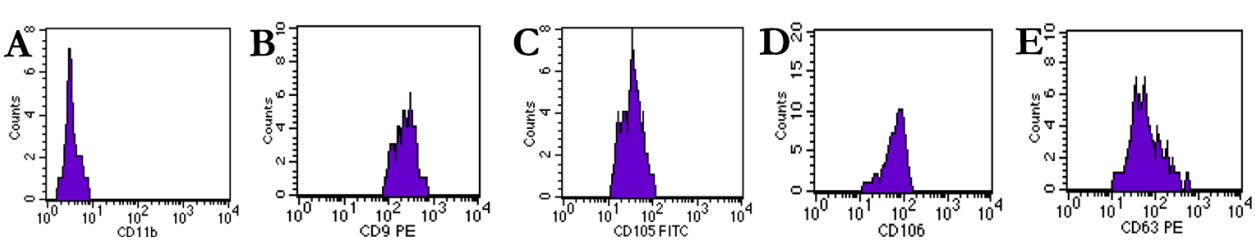

Figure 3: Showing representative histograms of flow cytometry analysis of neonatal LMSCs. (A) represented negative reaction with CD11b-PE (negative control). (B) Cells were stained by CD9-PE. (C) Cells were immunostained with CD105-FITC. (D) The histogram indicated positive cells for CD106-FITC. (E) Cells were immunostained with CD63-PE

Table 2: Absolute expression of desmin, nestin, and vimentin {no. of DNA copies log (10)} data expressed as Mean± SEM (Standard Error Mean) n=4. (F) referred to fetal and (P) referred to postnatal. Value carry * superscript indicated a significant difference $p < 0.01$

Genes \ Group	F group	P group	*P value*
Desmin	1.81±0.37	2.46±0.32	0.2552
Nestin	1.93±0.30	3.15±0.10*	0.018
Vimentin	3.05±0.16	3.34±0.61	0.669

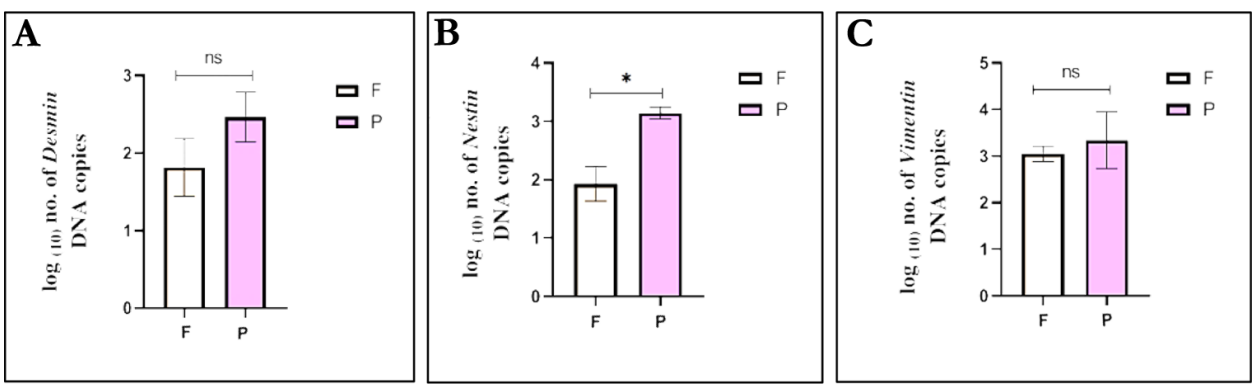

Figure 4: (A), (B), (C) Showing Absolute expression of desmin, nestin, vimentin respectively (no. of DNA copies log (10)) data expressed as Mean ± SEM n=4. (F) referred to fetal and (P) referred to postnatal, ns:non-significance, * indicated a significant difference

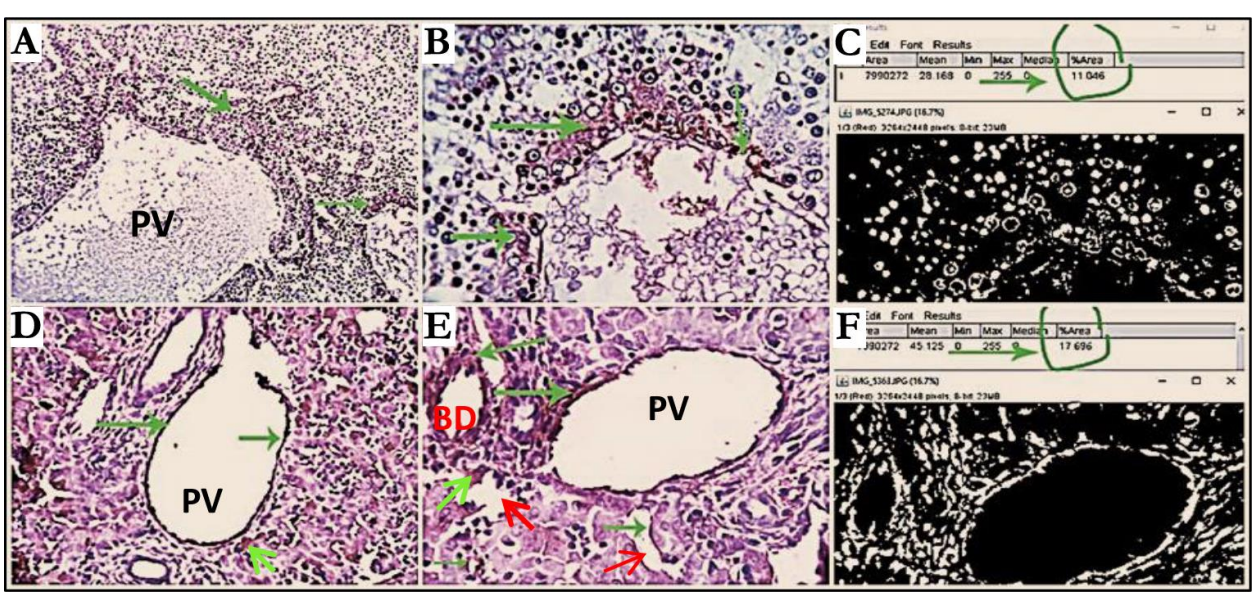

Figure 5: Prenatal (A, B) and postnatal (D, E) liver tissues, stained with CD105, showing a group of positive liver and vascular endothelial cells with moderate or intense brownish cytoplasmic reactivities (green arrows). The magnification power of (A) and (D) was 20x and of (B) and (E) was 40x. Estimated positive cells were seen in micrographs (C), (F), with the corresponding percentages of immune reactivity. PV: portal vein, BD: bile duct, red arrows: blood sinusoids

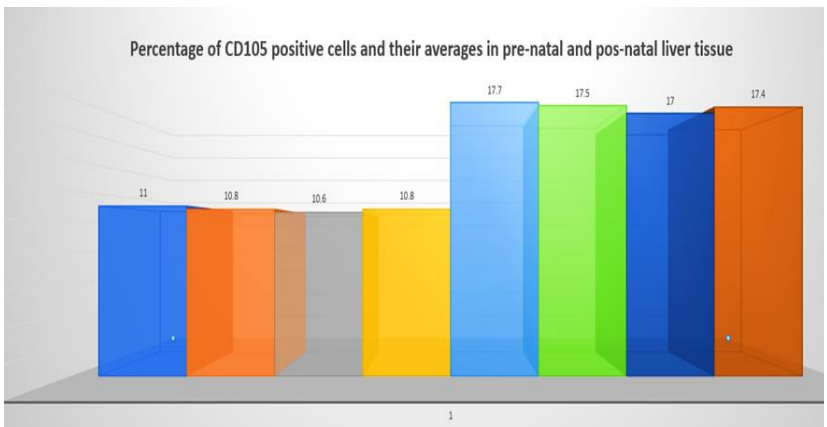

Figure 6: An illustrative chart demonstrating the percentage of positive CD105 cells and their averages in prenatal (first four columns) and postnatal (last four columns) liver tissues

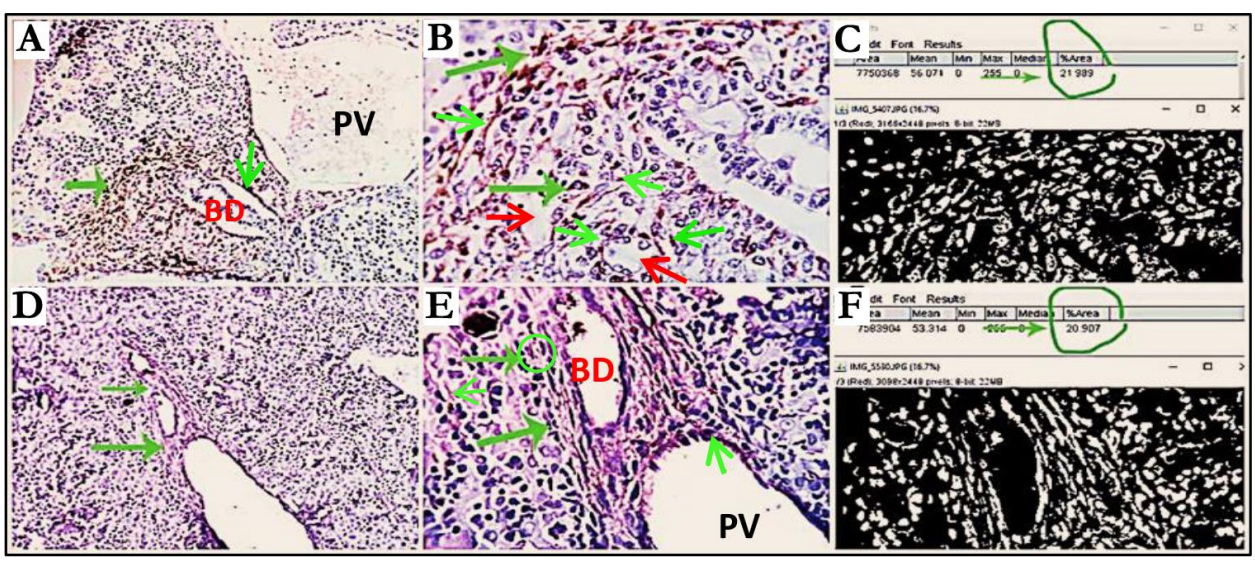

Figure 7: Prenatal (A, B) and postnatal (D, E) liver tissues, stained with desmin, showing a group of positive liver cells with moderate brownish cytoplasmic reactivities (green arrows). The magnification power of (A) and (D) was 20x and of (B) and (E) was 40x. Estimated positive cells were seen in micrographs (C), (F) with the corresponding percentages of immune reactivity. PV: portal vein, BD: bile duct, red arrows: blood sinusoids

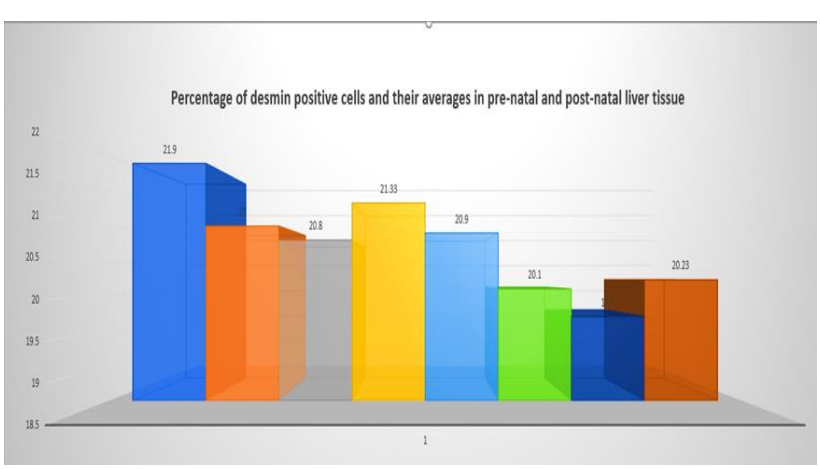

Figure 8: An illustrative chart demonstrating the percentage of positive desmin cells and their averages in prenatal (first four columns) and postnatal (last four columns) liver tissues

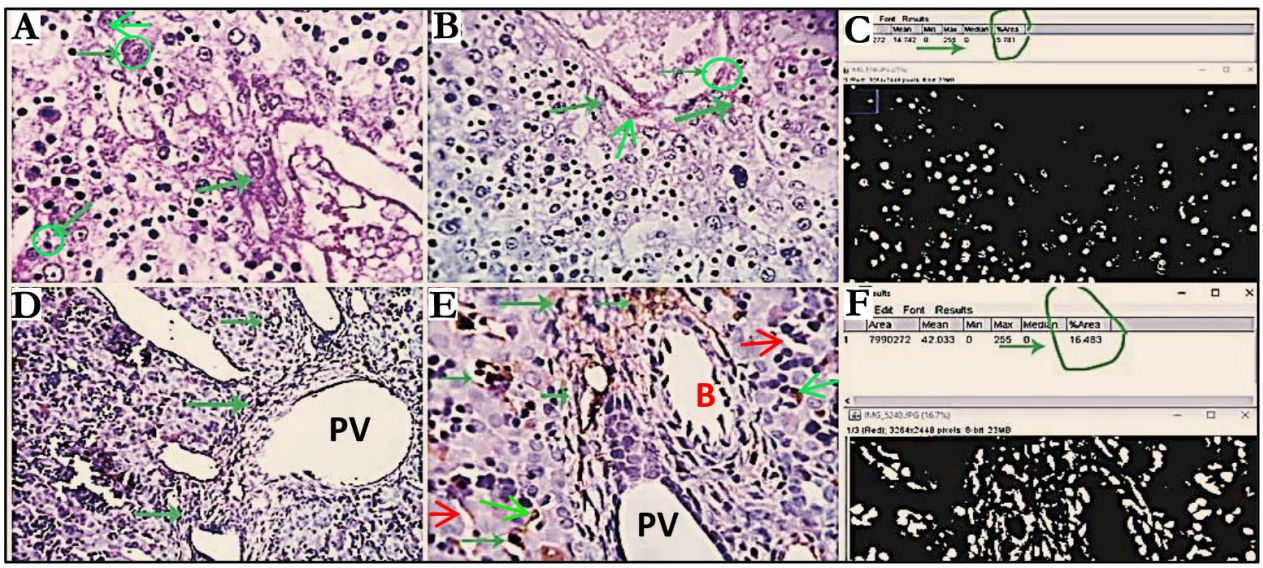

Figure 9: Prenatal (A,B) and postnatal (D,E) liver tissues, stained with vimentin, showing a group of positive liver cells with weak or moderate brownish cytoplasmic reactivities (green arrows). The magnification power of (A) and (D) was 20x and of (B) and (E) was 40x. Estimated positive cells were seen in micrographs (C) and (F), with the corresponding percentages of immune reactivity. PV: portal vein, BD: bile duct, red arrows: blood sinusoids

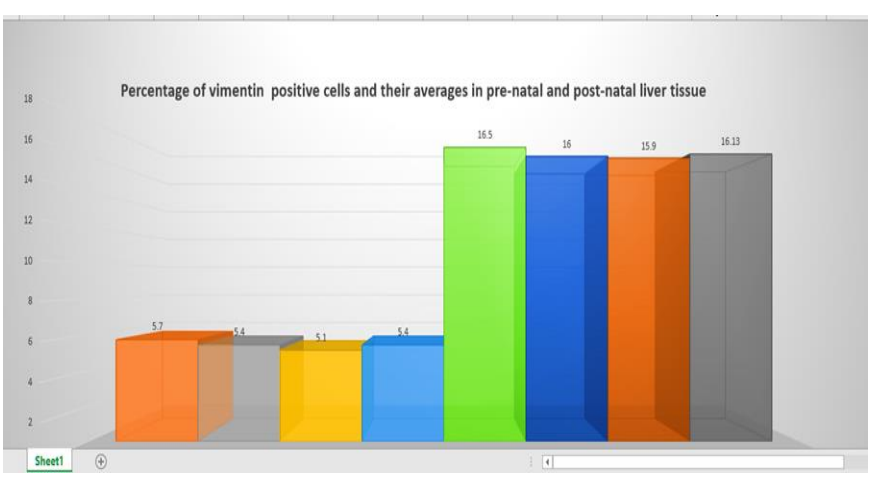

Figure 10: An illustrative chart demonstrating the percentage of positive vimentin cells and their averages in prenatal (first four columns) and postnatal (last four columns) liver tissues

Flow cytometry

Representative histograms (Figs. 2 and 3) showed staining profiles of LMSCs for specific antibodies. We stained LMSCs for mesenchymal specific markers; CD105 and CD106 in prenatal and postnatal livers. Positive expression of CD105 was in harmony with previous descriptions of (4) in rabbits, humans, and rats, besides (13) and (16) in humans. But there were some findings mentioned by (13) in rabbits cleared CD105 was absent from rabbit MSCs, besides (9) and (10) in humans. The positive expression of CD106 was similar to previous reports in humans (4). While (13) in rabbits disagreed with CD106 positive expression, they confirmed that CD106 was absent from the rabbit and human MSCs. Besides, (4) mentioned low expression of CD106 in the rats. CD63 and CD9 (Exosomal markers) were also expressed in fetal and neonatal LMSCs. Hematopoietic and endothelial markers; CD11b, CD38, and CD14 were negatively expressed in all populations of rabbit hepatic stem cells. In rabbits, (14) approved our results, besides (4), (13), and (10) in humans.qRT-PCR study

We used qRT-PCR analysis for the absolute expression of superscripts of vimentin, nestin, and desmin. Our result (Fig. 4) showed a significant difference between the expression of nestin

in prenatal and postnatal groups, while no significant difference between levels of both vimentin and desmin ($p<0.01$). Columns showed the combined mean values ($n = 4$) of fetal and neonatal rabbit LMSCs for each gene (Table 2). From the previously mentioned data, we could conclude that rabbit LMSCs expressed vimentin, nestin, and desmin. These results were in harmony with (14) who reported the presence of desmin and vimentin in rabbit MSCs but only vimentin expressed in human MSCs. Also (9) showed positive expression of vimentin in human MSCs. human MSCs were absent from desmin according to (15) outcomes. In humans, (10) found that MSCs expressed neither desmin nor vimentin.

Immunohistochemistry

CD105 was a type I membrane glycoprotein located on cell surfaces and had a crucial role in angiogenesis. Examined sections from fetal liver tissues treated with the mesenchymal angiogenetic marker CD105 revealed focal moderate brownish cytoplasmic reactivity in a group of undifferentiated mesenchymal cells of oval shapes around portal area and in a poorly differentiated vascular endothelium. Meanwhile postnatal liver tissue demonstrated markedly differentiated, strongly positive vascular and sinusoidal endothelial cells with a dark brownish cytoplasmic sustainability. These findings were in parallel with (17), (18) in humans. Positive cells were estimated using Image J software to be around 11-12% of fetal liver cells and 17-18% of neonatal liver cells (Fig. 5). An illustrative chart demonstrated the percentage of positive CD105 cells and their averages in fetal and neonatal liver tissues (Fig. 6).

Desmin was a muscle-specific member of the intermediate filament (IF). It was one of the earliest known myogenic markers in both skeletal muscle and heart. Examined sections from fetal liver tissues treated with the mesenchymal myogenic marker desmin revealed focal moderate brownish cytoplasmic reactivity in a group of undifferentiated oval and star-shaped mesenchymal cells. These cells were confined around the portal area, particularly at the vicinity of undifferentiated bile ducts. In humans, (19) proved our results. While (20) in rats and (19) in human noted that immunoreactivity of desmin gradually decreased upon reaching mid-gestation period. Neonatal liver tissue showed a remarkably differentiated cell with a moderate positive cytoplasmic reactivity to a group of aggregated spindle shaped mesenchymal cells (hepatic stellate cells). They were located around biliary and vascular structures (portal vein and hepatic artery) in the portal area and in some of the interstitial spindle cells. These findings were in accordance with those mentioned by (21) in dogs. On reviewing the latter mentioned data, we concluded that desmin (skeletal muscle marker) was also immuno-expressed in smooth muscles of bile duct and blood vessels wall. Our result was approved by (20) in rats. Positive cells were estimated using Image J software to be around 21-22% of fetal liver cells and 20-21% of neonatal liver cells (Fig. 7). An illustrative chart demonstrated the percentage of desmin positive cells and their averages in prenatal and postnatal liver tissues (Fig. 8).

Vimentin, also known as fibroblast intermediate filament, was the major intermediate filament found in non-muscle cells. These cell types include fibroblast, endothelial cells, macrophages, melanocytes, Schwann cells, and lymphocytes. Sections of fetal liver tissues treated with the vimentin (mesenchymal-fibrogenic marker) revealed focal weak brownish cytoplasmic reactivity in a group of undifferentiated mesenchymal cells. They are oval, flattened or rounded-shaped cells; located in sinusoidal cells (kupffer cells). In humans, (19) confirmed our results. While neonatal liver tissue showed remarkably differentiated cells with a moderate positive cytoplasmic reactivity to a group of spindle shape mesenchymal cells named as perisinusoidal cells (hepatic stellate cells). They were aggregated around the vascular structures in the portal area and in some of the sinusoidal endothelial cells. This outcome was in agreement with the findings of (21) in dogs and (22) in rabbits. The latter authors confirmed that the sinusoids and perisinusoidal cells were also stained for vimentin. Positive cells were estimated using Image J software to be around 5-6% of fetal liver cells and 16-17% of neonatal liver cells (Fig. 9). An illustrative chart demonstrated the percentage of vimentin positive cells and their averages in prenatal and postnatal liver tissues were demonstrated in (Fig. 10).

Conclusions

Immunophenotyping of Rabbit LMSCs was identified by flow cytometry. Fetal and neonatal livers were used here as a source of LMSCs. Both sources LMSCs showed positive expression of CD105 and CD106 but not expressed hematopoietic cells specific marker. qRT-PCR analysis for the absolute expression of vimentin, nestin, and desmin (cytoskeletons) in fetal and neonatal-MSCs was achieved. There was a significant difference between levels of expression of nestin in both groups of the study. We summarized the sites where LMSCs markers were expressed inside the liver tissue by the IHC technique to ensure the role of these cells in the developing liver. Our observations revealed the importance of the liver as a good source for the isolation of MSCs especially fetal LMSCs that showing superior expansion on culture. The latter point ensured the fetal LMSCs importance in organ transplantation.

Acknowledgments

This work was not funded. We also thank Department of Anatomy and Embryology, Zagazig University for their grateful help.

The authors declare no conflict of interest.

The supplementary data file is available upon reasonable request by e-mailing the corresponding authors.

References

1. McGeady TA, Quinn PJ, FitzPatric ES, Ryan MT, Kilroy D, Lonergan P. Veterinary Embryology textbook. 2nd edition, Pondicherry, India, 2017; 59-66.

2. Saliem M, Ericzon B, Ellis E, Hovatta O, Götherström C. Isolation and Characterization of Mesenchymal Stem Cells from Human Fetal Liver; Potential Candidates for Replacement Therapy in Liver Disease. J Liver: Dis Transplant 2012; 1 (2): 1-9.

3. Moreno R, Gonzalez IM, Rosal M, Farwati A, Gratacos E, Aran JM. Characterization of Mesenchymal Stem Cells Isolated from the Rabbit Fetal Liver, STEM CELLS AND DEVELOPMENT 2010; 19 (10): 1579-1588.

4. Lotfy A, Abdelsamed M, Abdelrahman A, Nabil A, Abdel-Fatah A, Hozayen W, Shiha G. Markers for the Characterization of Liver Mesenchymal Stem Cell. International Journal of Cell Science & Molecular Biology 2019; 6 (1): 116-121.

5. Curtis LAM, Wieczorek A J, McGann LE, Elliott JAW. Mesenchymal stromal cells derived from various tissues: Biological, clinical and cryopreservation aspects. Cryobiology 2015; 71(2):181-197.

6. Lu T, Hu P, Su X, Li C, Ma Y, Guan W. Isolation and characterization of mesenchymal stem cells derived from fetal bovine liver. Cell Tissue Bank 2014; 15: 439–450.

7. Kobolak J, Dinnyes A, Memic A, Khademhosseini A, Mobasheri A. Mesenchymal stem cells: Identification, phenotypic characterization, biological properties and potential for regenerative medicine through biomaterial micro-engineering of their niche. Methods 2016; 99: 62–68.

8. Ullah I, Subbarao RB, Rho GJ. Human mesenchymal stem cells - current trends and future prospective. Biosci Rep 2015; 35 (2): 1-18.

9. Dan YY, Riehle KJ, Lazaro C, Teoh N, Haque J, Campbell JS, Fausto N. Isolation of multipotent progenitor cells from human fetal liver capable of differentiating into liver and mesenchymal lineages. PNAS 2006; 103 (26): 9912–9917.

10. Turner R, Lozoya O, Wang Y, Cardinale V, Gaudio E, Alpini G, Mendel G, Wauthier E, Barbier C, Alvaro D, Reid LM. Human Hepatic Stem Cell and Maturational Liver Lineage Biology. Hepatology 2011; 53 (3): 1035–1045.

11. El-Kehdy H, Pourcher G, Zhang W, Hamidouche Z, Mainot SG, Sokal E, Charbord P, Najimi M, Kupperschmitt AD. Hepatocytic Differentiation Potential of Human Fetal Liver Mesenchymal Stem Cells: In Vitro and In Vivo Evaluation. Stem Cells International 2016; 1-12.

12. Moreno R, Gonzalez IM, Rosal M, Nadal M, Petriz J, Gratacos E, Aran JM. Fetal Liver-Derived Mesenchymal Stem Cell Engraftment After Allogeneic In Utero Transplantation into Rabbits. Stem cells and development 2012; 21(2), 284-295.

13. Nikoozad Z, Ghorbanian MT, Rezaei A. Comparison of the liver function and hepatic specific genes expression in cultured mesenchymal stem cells and hepatocytes. Iran J Basic Med Sci 2014; 17:27-33.

14. Lee TC, Lee TH, Huang YH, Chang NK, Lin YJ, Chien PWC, Yang WH, Lin MHC. Comparison of Surface Markers between Human and Rabbit Mesenchymal Stem Cells. PLOS ONE 2014; 9(11): 1-10.

15. Suzuki A, Zheng Y, Kaneko S, Onodera M, Fukao K, Nakauchi H,Taniguchi H. Clonal identification and characterization of self-renewing pluripotent stem cells in the developing liver. The Journal of Cell Biology 2002; 156 (1): 173–184.

16. Ghaneialvar H, Soltani L, Rahmani HR, Lotfi AS, Soleimani M. Characterization and Classification of Mesenchymal Stem Cells in Several Species Using Surface Markers for Cell Therapy Purposes, Ind J Clin Biochem 2018; 33(1): 46–52.

17. Theuerkauf I, Zhou H, Fischer HP. Immuno-

histochemical patterns of human liver sinusoids under different conditions of pathologic perfusion. Virchows Arch 2001; 438:498–504.

18. Yu D, Zhuang L, Sun X, Chen J, Yao Y, Meng K, Ding Y. Particular distribution and expression pattern of endoglin (CD105) in the liver of patients with hepatocellular carcinoma. BMC Cancer 2007; 7(122):1-10.

19. Gumerova AA, Titova MA, Kiassov AP. Expression of Different Liver Cell Markers during the Early Prenatal Human Development. CELL AND Tissue biology 2007; 1(2): 143–150.

20. Kiassov AP, Eyken PV, Pelt JFV, Depla E, Fevery J, Desmet VJ, Yap PSH. Desmin expressing non hematopoietic liver cells during rat liver development: An immuno-histochemical and morphometric study. Differentiation 1995; 59:253-258.

21. Milijana K, Gledic D, Kukolj V, Knezevic DJ, Jovanovic M, Bozic T, Sanja AK. Expression of α-SMA, Desmin and Vimentin in Canine Liver with Fibrosis. Acta Veterinaria (Beograd) 2009; 59 (4): 361-370.

22. Buyssens N, Kockx MM, Herman AG, Lazou JM, Berg KVD, Wisse E, Geerts A. Centrolobular Liver Fibrosis in the Hypercholesterolemic Rabbit. Hepatology 1996; 24(4): 939-946.